

In Vivo Diffusion Tensor Imaging of Rat Brain Acquired with a 3T Clinical MRI System and a High Strength Insert Gradient Coil

D. Mayer¹, E. Adalsteinsson^{2,3}, B. K. Rutt⁴, N. Zahr⁵, E. V. Sullivan⁵, A. Pfefferbaum^{5,6}

¹Radiology, Stanford University, Stanford, California, United States, ²Harvard-MIT Division of Health Sciences and Technology, Cambridge, MA, United States, ³Electrical Engineering and Computer Science, MIT, Cambridge, MA, United States, ⁴Imaging Research Laboratories, Robarts Research Institute, London, Ontario, Canada, ⁵Psychiatry & Behavioral Sciences, Stanford University, Stanford, CA, United States, ⁶Neuroscience Program, SRI International, Menlo Park, CA, United States

Introduction: Animal models of substance dependence can facilitate the identification of biological mechanisms underlying the predisposition, development, and maintenance of addiction. In vivo methods permit longitudinal study of the dynamic course of addiction and control of factors, such as aging, nutrition, substance consumption rate and amount, and age of onset, not possible in human study. Of particular relevance to human alcohol addiction is brain white matter, which postmortem study has shown is subject to myelin and cytoskeletal degradation¹ that may be reversible with abstinence.² In vivo human diffusion tensor imaging (DTI) studies of alcohol dependence provide evidence for microstructural disruption of white matter not detectible with bulk volume measures of conventional MRI.³ To date, DTI studies of the rodent brain have used high-field animal scanners (4.7-9.4T),⁴⁻⁶ and only a few have used in vivo methods.⁷ Here, we report on the development of an in vivo echo-planar (EP) DTI protocol with isotropic resolution on a 3T human MRI system equipped with a high-strength insert gradient coil for study of rat brain.

Methods: Healthy adult Wistar rats were scanned in 2-hour sessions. Anesthesia was provided by 2-3.5% isoflurane in oxygen (~2 l/min). Data were acquired on a clinical 3T GE Signa human MRI scanner equipped with a high-strength insert gradient coil (peak strength 600 mT/m, peak slew rate 3200 T/m/s, operating point: 500mT/m, 1800T/m/s)^{8,9} and a custom 44mm diameter quadrature birdcage coil. Imaging was accomplished with a modified GE product Echo-Planar DTI protocol (field-of-view (FOV)=32mm, TR/TE=2000/32.8ms). Magnet transaxial (rat anatomically coronal) isotropic data were acquired with 0.5mm slice thickness and 0.5mm in-plane resolution with partial k-space acquisition ($n_{read} = 64$, $n_{phase} = 48$) with and without diffusion weighting. Diffusion weighting ($\Delta=9ms$, $\delta=4ms$, $\epsilon=1ms$, $G=340mT/m$) was applied for b-value=1009 s/mm² in 6 noncollinear directions and the same 6 directions with opposite polarity to compensate for the diffusion effects of the imaging gradients.¹⁰ Crusher gradients were applied in x, y, and z immediately after the first and before the second diffusion lobe. The effect of the crusher gradients on diffusion weighting was neglected in the b-value calculation. The imaging sequence was preceded by a frequency selective lipid suppression module and an outer-volume suppression module. Saturation bands were placed at the left, right and bottom of the FOV. Frequency encoding direction was left to right. Data were acquired with a readout bandwidth of 200kHz ($G_{read}=147mT/m$) and echo spacing of 0.544ms in 26.1ms. Twenty-six slices with 16 averages per acquisition were collected, with the positive and negative polarity gradient scheme (7:36 min) repeated 6-12 times for a total acquisition time of ~46-92 min. After eddy-current correction,¹¹ fractional anisotropy (FA) and apparent diffusion coefficient (ADC) were computed by the method of Basser and Pierpaoli.¹² The genu of the corpus callosum and the anterior commissure were identified on midsagittal views of the FA data expanded 4 fold.

Results: The FA images had adequate signal-to-noise ratio (SNR) to detect rat brain white matter structures. The 92-min acquisition yielded mean FA of 52.2%±8.8SD (30.4-69.2%) in the callosal genu and 34.0%±5.0SD (18.8-42.0%) in the anterior commissure. Fig. 1 presents coronal, axial, and sagittal FA (left) and non-diffusion-weighted EP images (right) at the anterior commissure level. Fig. 2A presents coronal images at the genu level (EP images in column 1; FA images in column 2); columns 3-5 present the FA images with FA multiplied by the x (red), y (green) and z (blue) eigenvectors of the largest eigenvalue to demonstrate the primary orientation of the fibers. Fig. 2B presents the same scheme for a coronal image at the level of the anterior commissure.

Discussion and Conclusion: The high strength and speed of the insert gradient coil allowed for the strong diffusion gradients and the short readout time necessary to acquire high-resolution DTI in the rat brain on a human 3T scanner and to detect major white matter structures. The short readout time produced echo-planar DTI data without substantial B0 field inhomogeneity distortion. Longer scanning produced higher SNR and may enable fiber tracking and quantitative microstructural interrogation of white matter systems following exposure to neurotoxins, such as excessive alcohol ingestion or inhalation. A major advantage of employing insert gradient technology is the use of similar pulse sequences and field strength for preclinical and clinical research, thus enhancing the translational nature of such research.

Support: AA05965, AA12388, AA13521 (Integrative Neuroscience Initiative on Alcoholism—INIA)

References:

1. Harper C. *Neuropath Exp Neurol* 1998;57:101-110.
2. Pfefferbaum A, Sullivan EV et al. *Alc. Clin Exp Res*1995;19:1177-1191.
3. Pfefferbaum A, Sullivan EV. *Neuroimage* 2002;15:708-718.
4. Hoehn-Berlage M, Eis M, Schmitz B. *NMR Biomed* 1999;12:45-50.
5. Nair G, Tanahashi Y et al. *Neuroimage* 2005;28:165-74.
6. Zhang J, van Zijl PCM, Mori S. *NeuroImage* 2002;15:892-901.
7. Lin CY, Sun SW, Hong CY, Chang C. *Neuroimage* 2005;28:380-8.
8. Chronik B, Alejski A, Rutt BK. *Magma* 2000;10:131-146.
9. Chronik BA, Alejski A, Rutt BK. *Mag Res Med* 2000;44:955-963.
10. Neeman M, Freyer JP, Sillerud LO. *Mag Res Med* 1991;21:138-43.
11. Bodammer N et al. *Mag Res Med* 2004;51:188-193.
12. Basser PJ, Pierpaoli C. *J Mag Res. Series B* 1996;111:209-219.

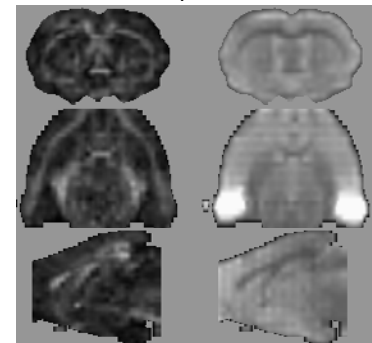


Fig. 1. FA (left) and non-diffusion EP images resliced in 3 planes at 46 min.

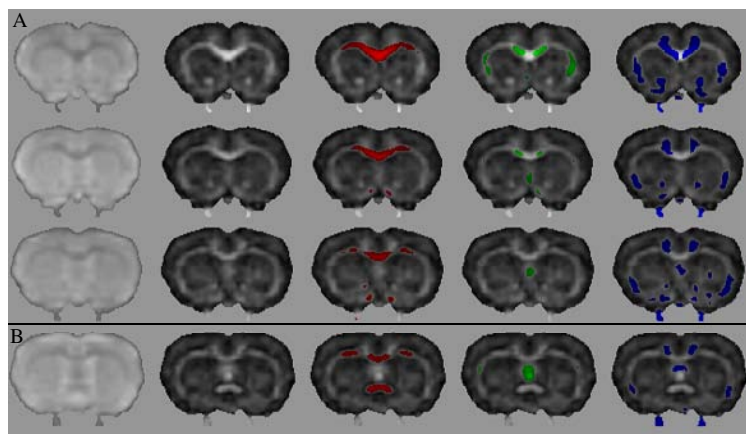


Fig. 2. b=0 EP images (left) and FA images (4 right columns) at 92 min.